Observational Study

Medicine®

OPEN

Ultrasound and radiological features of abdominal unicentric castleman's disease

A case series study

Kun Lv, MD, Yanan Zhao, MD, Wen Xu, MD, Chao Zhang, MD, Pintong Huang, MD*

Abstract

This study aimed to improve the diagnostic accuracy of abdominal unicentric Castleman's disease (UCD) by retrospectively summarizes the relatively specific imaging features of UCD.

This study retrospectively collected fifteen patients with abdominal UCD confirmed by pathology. All patients were underwent ultrasound (US), computed tomography (CT), or magnetic resonance imaging (MRI) examination. The imaging findings of UCDs were analyzed by senior radiologists.

Fifteen patients included 7 males and 8 females, aged 30 to 68 years old, with an average age of 51.73±13.57. In the 15 cases, 7 were located around the mesentery, 4 were located in the retroperitoneal space, and 4 in the liver. Fifteen cases contained solid masses, of which 13 had clear margins and 2 had blurred margins. The size of the mass ranged from 1.5 to 14.2 cm, with an average of 6.49±4.16 cm. US showed that 9 lesions were presented with hypo-echogenicity while 5 lesions presented with hyper-echogenicity spots. Unenhanced CT showed that the lesions were comprised of soft tissue while calcified lesions were found in 10 of the cases (66.67%, 10/15). T1-weighted imaging (T1WI) suggested the lesions as iso/hypo-signal, and mildly hyper-signal on T2-weighted imaging (T2WI). Diffusion-weighted imaging (DWI) showed different degrees of hyper-signal. Contrast-enhanced US and CT/MRI showed obvious enhancement at the arterial phase in 12 cases (85.71%, 12/14), most of which (50%, 7/14) showed continuous enhancement at the delayed phase. Feeding vessel could be seen within, or around the lesion in 5 cases (35.71%, 5/14).

The study suggests that abdominal UCD commonly manifests as well-defined, homogeneous, solid, and hypervascular masses. Calcification and the presence of feeding vessel in the tumors are relatively specific features of abdominal UCD.

Abbreviations: ADC = apparent diffusion coefficient, CT = computed tomography, DWI = diffusion weighted imaging, GIST = gastrointestinal stromal tumor, HV = hyaline vascular, MRI = magnetic resonance imaging, PC = plasma cell, T1WI = T1-weighted imaging, T2WI = T2-weighted imaging, UCD = unicentric Castleman's disease, US = ultrasound.

Keywords: castleman's disease, CT, MRI, ultrasound

1. Introduction

Castleman's disease (CD), also known as Giant Lymph Node Hyperplasia and Follicular Lymphoid Tissue Hyperplasia, is a rare proliferative disease of the lymphoid tissue. It was first described by Castleman in 1954[1] and most commonly present in the chest and neck lymph nodes. The disease is divided into two major types: unicentric CD (UCD) and multicentric CD (MCD). The occurrence of UCD in the abdomen is quite rare.[2] Moreover, abdominal UCD is easily misdiagnosed as other hypervascular tumors, such as gastrointestinal stromal tumor (GIST) or lymphoma, etc. Since the treatment paradigm varies significantly depending on the differential diagnosis, an accurate method to diagnose CD versus other similar ailments is important for guiding treatment and improving prognosis. Compared with magnetic resonance imaging (MRI) and computed tomography (CT), ultrasound (US) is a lower cost, portability and non-invasive tool without ionizing radiation damage and has been widely used in the diagnosis and evaluation of diseases, included in the evaluation of nerve entrapment syndromes and assessing musculoskeletal disorders.[3,4] Yet, there are few reports on abdominal CD imaging and most of them being case reports, especially the reports of US on CD. Current

Editor: Oguzhan Ekizoglu.

The study was supported by the Natural Science Foundation of Zhejiang Province grant: LY16H180005.

The authors have no conflicts of interest to disclose.

The datasets generated during and/or analyzed during the current study are available from the corresponding author on reasonable request.

Department of Ultrasound Medicine, The Second Affiliated Hospital of Zhejiang University School of Medicine, Hangzhou, P.R. China.

** Correspondence: Pintong Huang, Department of Ultrasound Medicine, The Second Affiliated Hospital of Zhejiang University School of Medicine, 88 Jiefang Road, Shangcheng District, Hangzhou 310009, P.R. China (e-mail: huangpintong@zju.edu.cn).*

How to cite this article: Lv K, Zhao Y, Xu W, Zhang C, Huang P. Ultrasound and radiological features of abdominal unicentric castleman's disease: A case series study. Medicine 2020;99:18(e20102).

Received: 5 November 2019 / Received in final form: 1 April 2020 / Accepted: 2 April 2020

http://dx.doi.org/10.1097/MD.0000000000020102

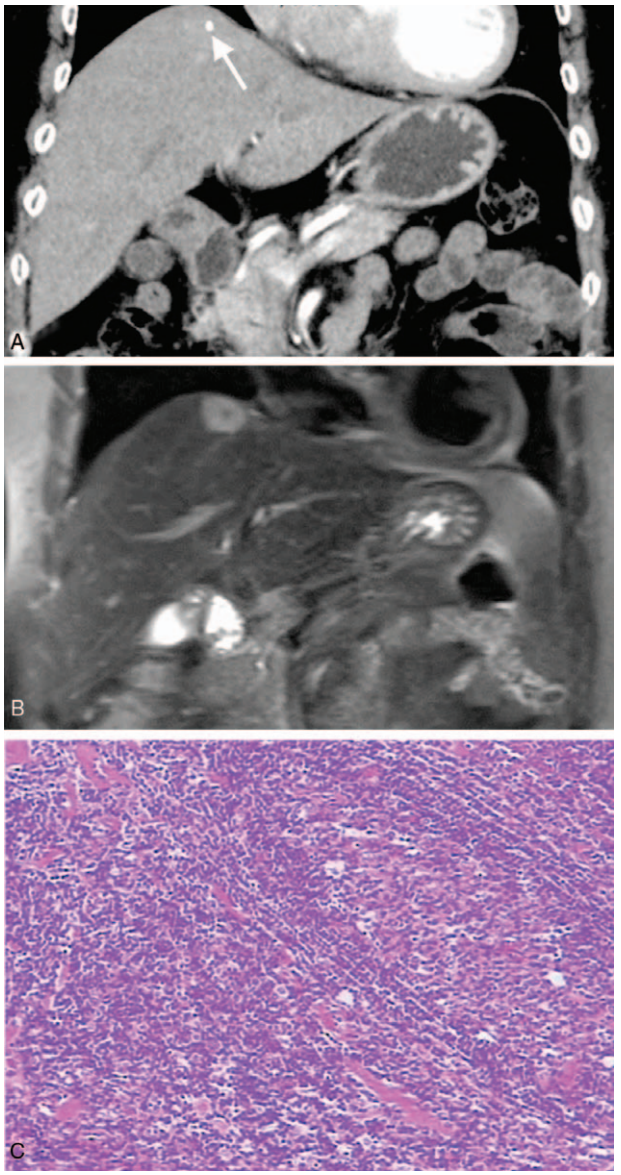

Figure 1. Case 1: Hepatic CD in an asymptomatic 68-year-old woman. Coronal CT showed continuous enhancement of hepatic nodules at the parenchymal stage (A), with punctate calcification in the lesion (arrow); coronal T2WI showed hepatic nodules with hyper-signal and punctate hypo-signal (B); pathology showed a large number of lymphocytes arranged in concentric circles (C, HE × 200).

epidemiological data and improvement of detection rate suggests that the incidence of CD is increasing.[5,6] In light of this, 15 cases of abdominal CD with complete clinical data were collected. Their ultrasonographic and radiological features were retrospectively analyzed to improve the understanding of CD imaging features to improve the accuracy of diagnosis (Figs. 1–3).

2. Material and methods

The institutional review board of The Second Affiliated Hospital of Zhejiang University School of Medicine approved this retrospective study and waived informed consent.

The inclusion criteria included

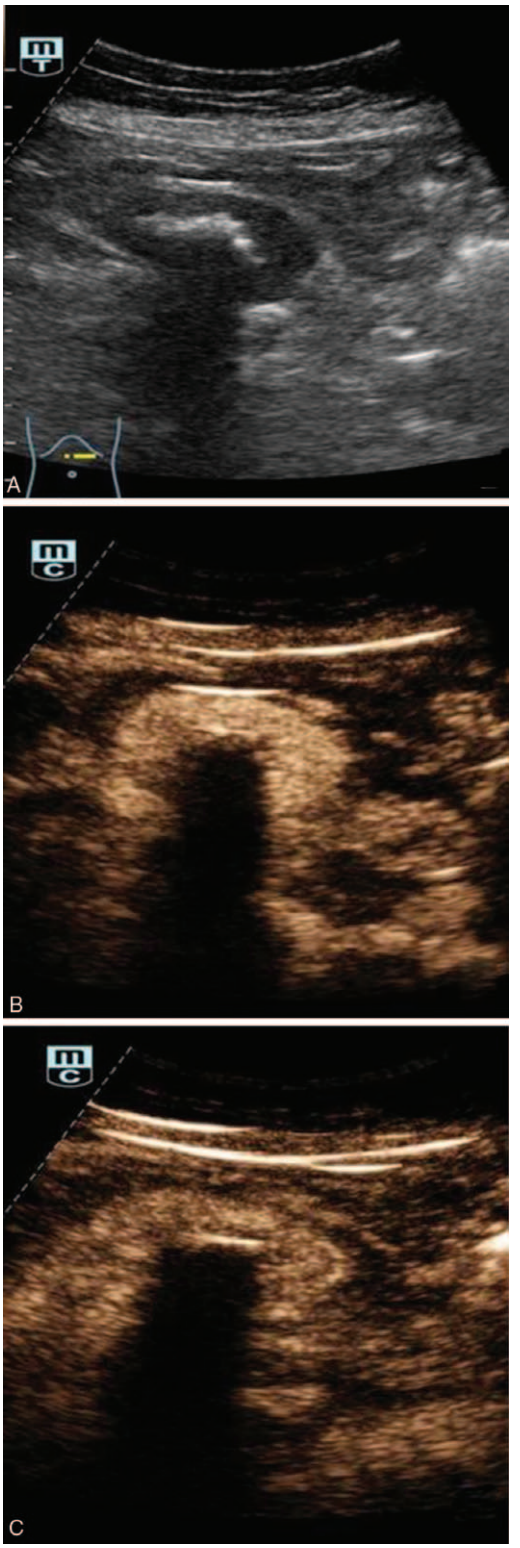

Figure 2. Case 2: Perimesenteric CD of US findings in an asymptomatic 63-year-old woman. Two-dimensional US showed hypo-echogenicity masses with hyper-echogenicity spots (A). CEUS of the mass showed hyperenhancement of the mass at 19 seconds (B) and continuous enhancement at 1 min 40 s (C).

1. CD was confirmed by pathology;
2. the patients with high quality images of US, CT, or MRI;
3. the patients with complete clinical data.

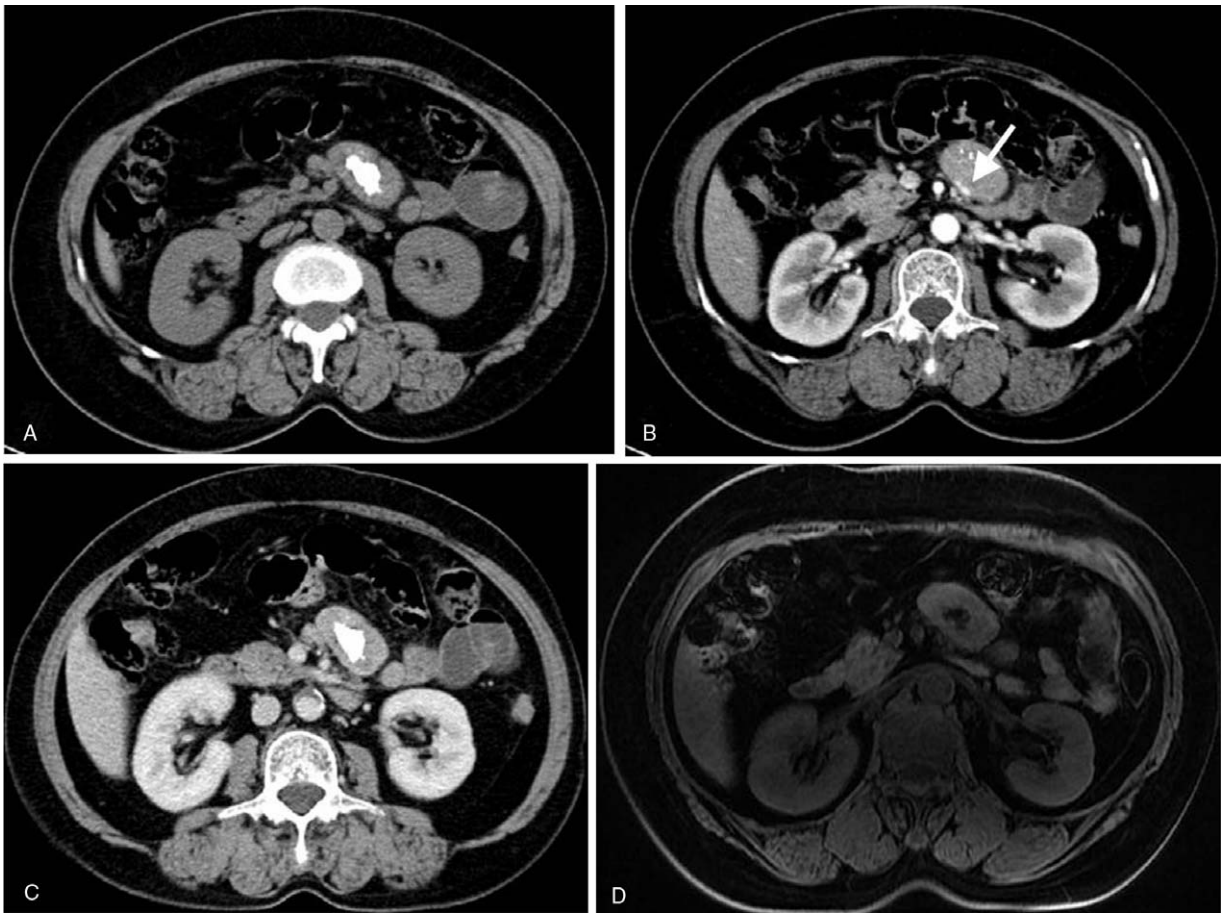

Figure 3. Case 2: Perimesenteric CD of CT and MRI findings in an asymptomatic 63-year-old woman. Unenhanced CT showed a perimesenteric mass with nodular calcification in the abdomen (A). Contrast-enhanced CT showed arterial enhancement of the mass, feeding vessel (B, arrow) could be seen in the lesion, and continuous enhancement at the delayed phase (C). T1WI showed iso/hypo-signal (D), T2WI showed mild hyper-signal, contrast-enhanced MRI showed the mass with an obvious enhancement at the arterial phase (E) and continuous enhancement at the delayed phase (F). DWI showed a hyper-signal region (G) and the ADC value was low (H). Pathology showed a large number of lymphocytes (I, HE × 200).

None of the three were excluded. According to these criteria, the study collected 15 CD patients from 2005 to 2019. All patients with CD were confirmed by pathology, including 7 males and 8 females, aged 30 to 68 years, with an average age of 51.73 ± 13.57 years old. Two patients were treated for abdominal pain, 1 for poor appetite, and 12 for no obvious discomfort. US, CT, or magnetic MRI were performed in all 15 patients, of whom 9 cases underwent US, 15 underwent CT and 3 underwent MRI. All US, CT, and MRI images of UCDs were analyzed by the senior radiologists. Characteristics include the boundary, shape, internal echo of US, density of CT and signal of MRI and enhancement of each imaging modalities of UCDs were analyzed.

3. Results

The clinical data and imaging findings were summarized in Table 1. All 15 cases underwent surgery and pathological examination, revealing a hyaline vascular (HV) subtype for all samples. Of the 15 cases, 7 were located around the mesentery, 4 in the retroperitoneal space, and 4 in the liver. All 15 cases contained a single localized mass, of which 13 had clear margins and 2 had blurred margins. The size of the masses ranged from 1.5 to 14.2 cm, with an average of 6.49 ± 4.16 cm. US showed that 9 lesions were presented with hypo-echogenicity while 5 lesions presented with hyper-echogenicity spots. CT examination was performed in all 15 cases. Unenhanced CT revealed the masses as being comprised of soft tissue while 10 cases (66.67%, 10/15) displayed evidence of calcification. Five cases were found to be heterogeneous in composition, and the diameters were larger than 8 cm. Three cases underwent MRI examination. The lesions presented as iso-hyposignal on T1-weighted imaging (T1WI) and iso-hypersignal on T2-weighted imaging (T2WI). Diffusion-weighted imaging (DWI) showed different degrees of hyper signal. Fourteen cases were underwent contrast enhanced (CE) US, CT/MRI. Most of cases (85.71%, 12/14) showed obvious enhancement in the arterial phase, and continuous enhancement (50%, 7/14) at the delayed phase on CEUS or CECT/CEMRI. Feeding vessel could be seen within, or around the lesion in 5 cases (35.71%, 5/14). The pathology showed the lesions were composed of abundant lymphocytes and hyalinized vessels, which further confirms that the 15 cases were of the HV subtype.

4. Discussion

Castleman's Disease (CD), also known as macro-lymph node hyperplasia and follicular lymphoid tissue hyperplasia, is a rare

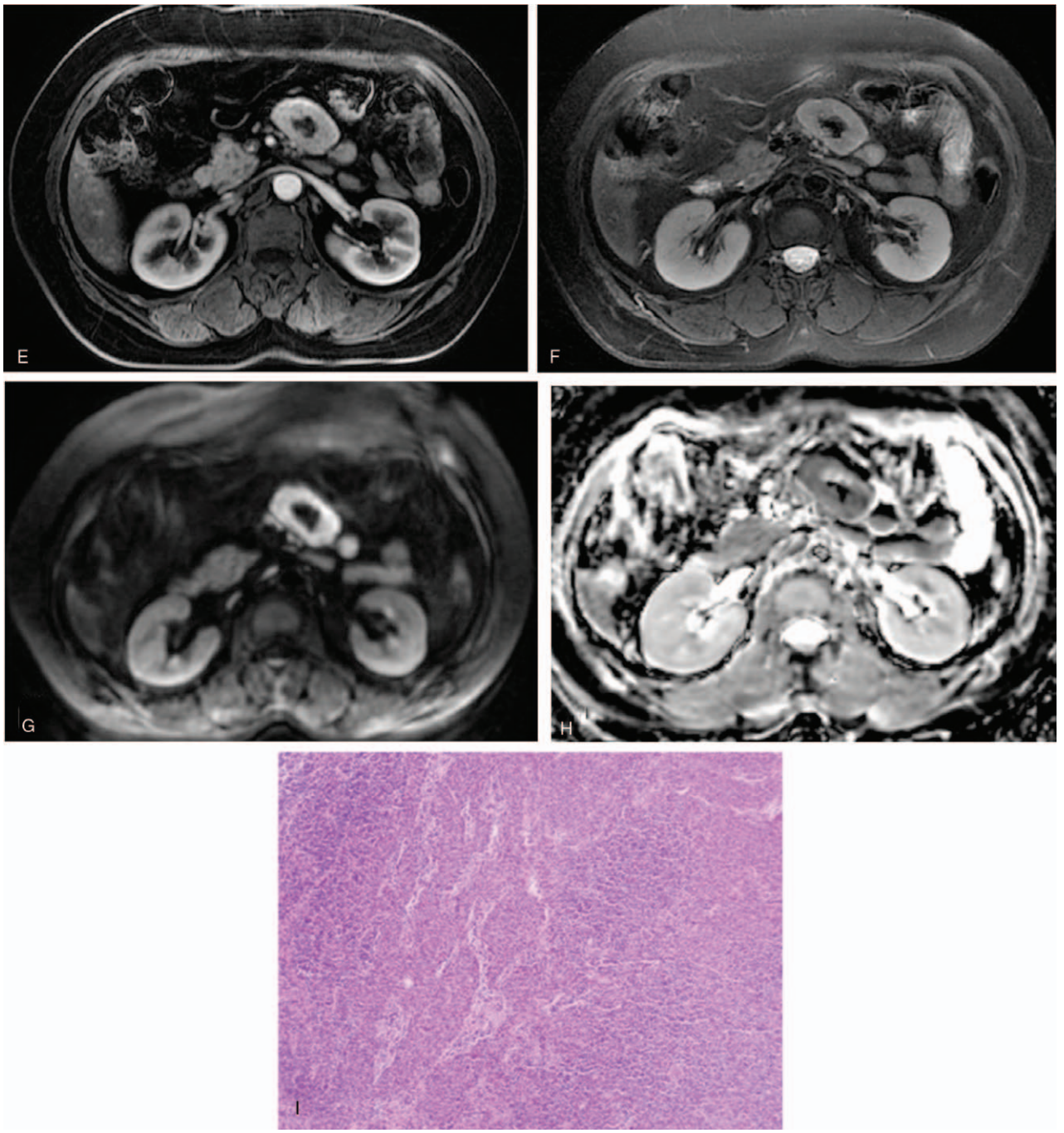

Figure 3. (Continued).

lymphoid tissue proliferative disease. The etiology of the disease is unknown, which is often associated with viral infection or immunomodulatory disorders. The roles of interleukin 6 and human herpesvirus 8 in CD have been well described.[7] Tumors may occur in any part of the lymphoid tissue, but they are more common in the chest and neck than in the abdomen. According to the histological characteristics, tumors can be divided into either hyaline vascular (HV) or plasma cell (PC) subtypes, with mixed variants between them.[8] Clinically, according to the extent of lesion involvement, the lesions can be divided into unicentric CD (UCD) and multicentric CD (MCD). UCD is a focal lesion, and most of them are of the HV type. Typically, women aged 30 to 40 years present more commonly, accounting for about 90% of cases. Specimen findings include intra and interfollicular hyaline capillary hyperplasia, and interfollicular lymphoid tissue hyperplasia. Histologically, small lymphocytes in the cuff area are arranged in concentric circles about the germinal center. A small number of plasma cells are often seen between the follicles. Typically, the prognosis for patients improves after surgical removal. While most subtypes present with no obvious symptoms, local symptoms, if present, often relate directly in severity to the size and location of the mass. Most cases of MCD

Table 1

Clinical data and imaging features of abdominal unicentric Castleman's disease (15 cases).

Cases	Sex/age	Location	Symptom	Size (cm)	Imaging features			Pathology
					Margin	Ultrasound	CT/MRI	
1	F/56	Liver	Abdominal pain	3.5	Well-defined	Hypoechoic	Hyper and continuous enhancement	HV
2	F/68	Liver	Asymptomatic	1.5	Well-defined	Hypoechoic	Hyperenhancement	HV
3	F/64	Liver	Asymptomatic	1.6	Well-defined	Hypoechoic	Hyperenhancement, diffusion restricted	HV
4	M/55	Retroperitoneum	Asymptomatic	8.0	Blurred	Heterogeneous, hypoechoic, calcifications, hypervascular	Heterogeneous, hyper and continuous enhancement, calcifications	HV
5	M/55	Perimesenteric	Asymptomatic	6.0	Well-defined	Hypoechoic, hypervascular	Hyper and continuous enhancement	HV
6	F/50	Retroperitoneum	Abdominal pain	13.0	Well-defined	NA	Heterogeneous, hyperenhancement, calcifications, feeding vessel	HV
7	F/34	Retroperitoneum	Asymptomatic	13.1	Well-defined	NA	Heterogeneous, calcifications, feeding vessel	HV
8	M/41	Perimesenteric	Asymptomatic	6.0	Well-defined	NA	Calcifications, mild and continuous enhancement, feeding vessel	HV
9	M/57	Perimesenteric	Asymptomatic	5.4	Lobulated	NA	Hyperenhancement, feeding vessel	HV
10	M/36	Perimesenteric	Asymptomatic	6.7	Well-defined	Hypoechoic, calcifications	Hyperenhancement, calcifications	HV
11	M/30	Retroperitoneum	Asymptomatic	14.2	Blurred	NA	Heterogeneous, hyperenhancement, calcifications	HV
12	F/33	Perimesenteric	Poor appetite	8.2	Well-defined	Hypoechoic, calcifications, hypervascular	Heterogeneous, hyper and continuous enhancement, calcifications	HV
13	M/66	Perimesenteric	Abdominal pain	2.9	Well-defined	Hypoechoic, calcifications	Calcifications	HV
14	F/63	Perimesenteric	Asymptomatic	5.0	Well-defined	Hypoechoic, calcifications, hyper and continuous enhancement	Hyper and continuous enhancement, calcifications, diffusion restricted, satellite nodules, feeding vessel	HV
15	F/68	Liver	Asymptomatic	2.3	Well-defined	NA	Hyper and continuous enhancement, calcifications, diffusion restricted	HV

CT = computed tomography, F = female, HV = hyaline-vascular, M = male, MRI = magnetic resonance imaging, NA = not available.

are of the PC subtype, commonly seen in 50 to 60-year-old patients. The disease is systemic, accounting for about 10% of the disease and often accompanied by fever, weight loss, night sweats, arthralgia. and hepatosplenomegaly. There are normal to enlarged follicular central cells and abundant mature plasma cells. Vascular proliferation is less common. Systematic treatment, including hormone or immunosuppressive agents, can be used for treatment but the prognosis is often poor. In this study, all 15 cases were of single masses; all of which were of the HV type. Among them, 11 cases were found incidentally by physical examination or other examinations, 3 cases were diagnosed with abdominal pain and 1 case was diagnosed with poor appetite.

The imaging manifestations of CD are related to the pathological classification. The HV type usually presents as a round, or lobulated soft tissue mass with clear margins, less cystic degeneration and less necrosis.[9] Unenhanced CT revealed a homogenous region of iso/hypo-density. Meanwhile, MRI examination showed a homogenous iso/hypo-signal on T1WI and hyper-signal on T2WI. DWI revealed an overall hyper-signal and a low apparent diffusion coefficient (ADC) value, which indicated the lesions provided some limitation of diffusion. These results confirm that the lesion is composed of multiple, rapidly proliferating cell.[10] On contrast-enhanced CT/MRI, the lesions showed obvious enhancement, along with an abnormal strip-like vascular shadow.[11] This finding may be related to the rich blood supply of tumors, strong collateral circulation, and lymphoid follicular tissue. In this group, 14 cases underwent a contrast CT scan, and 12 cases agreed with the aforementioned findings, 1 case showed only mild enhancement, and 5 cases revealed feeding vessel within, or around the lesion. In masses >5 cm, necrosis or fibrosis may occur. These lesions tend to have a heterogeneous enhancement with a central region of low-attenuation.[12] In this group, 5 cases showed obvious heterogeneous enhancement, and the maximum length was >8 cm. Three cases underwent MRI examination, which also agreed with the aforementioned findings. Furthermore, polymorphic (punctate, branched, etc.) calcification is often seen in the lesion.[13] This may be due to the thickening of the proliferative capillary wall, accompanied by hyaline degeneration, fibrinolysis, and degeneration of other connective tissues. Specifically, 10 cases revealed single or multifocal calcifications, which is consistent with the previous studies. As evidenced by the aforementioned results, the imaging findings of MCD are complex and variable.[14] Yet, almost all examples of MCD showed multiple enlarged lymph nodes with uniform density. The homogenous density is mainly due to large follicles and plasma cell infiltration between follicles, resulting in lower vascular proliferation. If MCD is of the HV type, its enhancement is similar to that of UCD. All cases collected in this study were of the UCD HV type. The imaging characteristics of PC type CD need to be further collected and analyzed in the later stage.

At present, there are only a few reports on the diagnosis of CD by US. In this group, 9 cases underwent ultrasound examination and 1 case underwent a CEUS. Two-dimensional US showed that

all lesions manifest as hypo-echogenicity masses, including 5 cases with hyper-echogenicity calcification, 4 cases with abundant blood flow signals, and 1 case with CEUS that showed obvious enhancement and continuous enhancement. Based on the ultrasonographic findings in the literature and the cases in this group, the characteristics of the HV type were summarized as follows:

1. the majority of lesions were single lesions;
2. most lesions were round or quasi-circular, with clear margins;
3. most lesions were homogeneously hypo-echogenicity with good transmissivity;
4. hyper-echogenicity calcification was commonly seen;
5. color doppler flow imaging revealed ample blood flow; and
6. CEUS showed obvious enhancement and continuous enhancement.

CD lacks characteristic clinical manifestations, especially in the high proportion of HV type. Although imaging can be used to assist in visualizing CD, qualitative diagnosis is difficult, especially in the abdominal and pelvic regions, which need to be differentiated from other abdominal hypervascular lesions. For instance, hepatic masses need to be differentiated from hepatocellular carcinoma (HCC), adenoma, focal nodular hyperplasia (FNH), and hepatic hemangioma by combining the corresponding clinical manifestations, laboratory examinations and specific imaging findings.[15] Cholangiocarcinoma can also form a hypervascular mass but is generally associated with biliary dilatation.[16] When the mass is located in the perimesenteric or retroperitoneal space, it needs to be differentiated from stromal tumors, neurogenic tumors, lymphomas, lymph node tuberculosis, sarcomas, etc. The imaging manifestations of lymph node tuberculosis are diverse due to the different pathological changes, which need to be combined with clinical manifestations. As many patients show similar radiologic features, a differential diagnosis is difficult to arrive at. If the lesion presents as an isolated mass with a similar appearance to benign tumors in the abdomen and pelvis, CD should be taken into consideration. This is especially true if the lesion is presented as hypervascular, calcified or feeding vessel.

The diagnosis of CD mainly relies on imaging modalities such as US and CT/MRI. Smaller lesions are more difficult to visualize on US due to gas interference in the abdominal cavity. Therefore, CT/MRI would be more appropriate. Yet, US offers a versatile and rapid diagnosis of larger lesions. In a patient with systemic symptoms and abnormal labs, the PC subtype should be considered. Imaging of other relevant anatomical regions should also be carried out in the clinic due to the risk of multiple lesions.

5. Conclusion

In conclusion, the imaging features of abdominal UCD share key characteristics. Specifically, abdominal UCD lesions are commonly described as single, soft tissue masses with clear margins and an obvious homogenous enhancement on contrast imaging. Some lesions may also present as calcifications and feeding vessel in, or around the central mass. These parameters, with relative specificity, are helpful in the differential diagnosis of UCD from other diseases. While US, CT, and MRI are indispensable in the diagnosis of UCD, the gold-standard still relies on pathological and immunohistochemical analysis for confirmation.

Author contributions

All authors contributed to this paper; PTH designed the outline for the study; KL acquired the data, and wrote the paper; YNZ and WX offered assistance for correct the syntax errors of the paper. PTH, YNZ, WX, CZ and KL revised and edited, and all authors approved the final version.

References

[1] Castleman B, Towne VW. Case records of the Massachusetts general hospital; weekly clinicopathological exercises; founded by Richard C. Cabot. N Engl J Med 1954;251:396–400.
[2] Ferreira Junior EG, Apolinario Costa P, Freire Golveia Silveira LM, et al. Localized pancreatic Castleman disease presenting with extrahepatic dilatation of bile ducts: a case report and review of published cases. Int J Surg Case Rep 2019;54:28–33.
[3] Wu WT, Chang KV, Mezian K, et al. Basis of shoulder nerve entrapment syndrome: an ultrasonographic study exploring factors influencing cross-sectional area of the suprascapular nerve. Front Neurol 2018;9:902.
[4] Chang KV, Yang KC, Wu WT, et al. Association between metabolic syndrome and limb muscle quantity and quality in older adults: a pilot ultrasound study. Diabetes Metab Syndr Obes 2019;12:1821–30.
[5] Guazzaroni M, Bocchinfuso F, Vasili E, et al. Multicentric Castleman's disease: report of three cases. Radiol Case Rep 2018;14:328–32.
[6] Bracale U, Pacelli F, Milone M, et al. Laparoscopic treatment of abdominalunicentric castleman's disease: a case report and literature review. BMC Surg 2017;17:38.
[7] Polizzotto MN, Uldrick TS, Wang V, et al. Human and viral interleukin-6 and other cytokines in Kaposi sarcoma herpesvirus-associated multicentric Castleman disease. Blood 2013;122:4189–98.
[8] Soumerai JD, Sohani AR, Abramson JS. Diagnosis and management of Castleman disease. Cancer Control 2014;21:266–78.
[9] Zhou LP, Zhang B, Peng WJ, et al. Imaging findings of Castleman disease of the abdomen and pelvis. Abdom Imaging 2008;33:482–8.
[10] White NS, McDonald C, Farid N, et al. Diffusion-weighted imaging in cancer: physical foundation and application of restriction spectrum imaging. Cancer Res 2014;74:4638–52.
[11] Jiang XH, Song HM, Liu QY, et al. Castleman disease of the neck: CT and MR imaging findings. Eur J Radiol 2014;83:2041–50.
[12] Madan R, Chen JH, Trotman-Dickenson B, et al. The spectrum of Castleman's diseases: mimics, radiologic correlation and role of imagine. Eur J Radiol 2012;81:123–31.
[13] Bonekamp D, Horton KM, Hruban RH, et al. Castleman disease: the great mimic. Radiographics 2011;31:1793–807.
[14] Johkoh T, Müller NL, Ichikado K, et al. Intrathoracic multicentric Castleman disease: CT findings in 12 patients. Radiology 1998;209: 477–81.
[15] Peck D, Lum PA. Castleman disease in the porta hepatis: biphasic helical computed tomography. Can Assoc Radiol J 1996;47:410–2.
[16] Chung YE, Kim MJ, Park YN, et al. Varying appearances of cholangiocarcinoma: radiologic-pathologic correlation. Radiographics 2009;29:683–700.